

On the colors of distant objects

David K. Lynch and S. Mazuk

Distant objects like clouds, mountains, and the Sun can appear to have colors that are significantly different from their intrinsic colors: the low Sun is often red, white clouds and snow-capped peaks appear yellow or pink, and dark green or gray mountains can appear blue or purple. The color alteration increases with distance, or alternatively, optical depth. We investigate the perceived colors of distant objects by computing the CIE chromaticity coordinates from their spectra. For sources viewed through significant amounts of atmosphere (e.g., the low Sun), MODTRAN4 radiative-transfer calculations are used to retrieve the spectra. In addition to clouds and mountains, the colors of stars, the Sun, and the sky are presented as a function of solar elevation under a variety of atmospheric conditions. © 2005 Optical Society of America

OCIS codes: 010.1290, 290.1310, 290.2200, 290.5870, 330.1720.

1. Introduction

Two processes modify the colors of distant objects: (1) extinction attenuates the object's light, and (2) scattering of sunlight by atmospheric molecules and aerosols adds light along the observer's line of sight ("airlight").¹⁻³ Both processes are wavelength dependent. All calculations presented in this paper are appropriate for single scattering, which dominates many and perhaps most optical effects in the atmosphere. An excellent discussion of multiple scattering can be found in a paper by Bohren.⁴

Limiting cases provide insight into how and why color is changed. A black object will appear to get brighter and bluer with increasing distance as Rayleigh scattering introduces airlight into the beam. At extremely large distances, the only light perceived by the observer is airlight. The blackness of space seen through the atmosphere is a good example: it's not black, it's sky blue. Near the horizon, the sky's blue color approaches white because of multiple scattering (and in practice, sunlight scattered by aerosols), a limiting case of color change with distance for a very dark or black object. The other limiting case is a white object. Rayleigh scattering and absorption by water vapor cause it to take on warm color, i.e., yellow or red. The best example is the Sun or full moon. As it

approaches the horizon, it begins to yellow. Thus an object's apparent color is determined by its initial brightness and color, and the opposing mechanisms of airlight, which pulls the color toward the blue, and atmospheric extinction, which pulls the object's color toward the red.

The Commission Internationale De L'Eclairage (CIE) chromaticity system⁵ makes a quantitative link between a source's radiometric spectra (e.g., $W \text{ cm}^{-2} \text{ nm}^{-1}$) and its perceived color. A useful aspect of the system is that it shows how sources with different spectral energy distributions can, in many circumstances, produce identical physiological responses. However, the CIE system was not intended to quantify perception of colors in the broadest sense. It was developed for commercial applications as an aid to color matching of paints and dyes viewed under controlled conditions. The developers of the CIE system repeatedly and explicitly stated that it cannot and should not be used to predict color appearance. For the latest on color appearance models, see Fairchild.⁶ We are not claiming to predict in an absolute sense the perceived colors of distant objects. We are attempting to set the stage for future color perception studies by providing realistic radiometrically accurate spectra and showing how they transfer to the CIE color system. Perhaps more important than the actual CIE coordinates are the *changes* in the coordinates as a function of the various parameters of the spectra.

The conversion of radiometric spectra to CIE x - y coordinates is a straightforward integral of the product of the three tristimulus curves with the spectrum

D. K. Lynch (thule@earthlink.net) is with Thule Scientific, 22914 Portage Circle Drive, Topanga, California 90290.

Received 1 February 2005; revised manuscript received 26 April 2005; accepted 29 April 2005.

0003-6935/05/275737-09\$15.00/0

© 2005 Optical Society of America

of the source in question. Perfect “white” is defined here as $x = 0.333$ and $y = 0.333$, though other definitions are possible. We shall use the 1931 coordinate system rather than the 1976 system because the former is more familiar to most scientists and engineers.

Our goal here is to quantitatively explain the changes in the spectra of distant objects and to relate them to the color perceived by an observer. Of particular interest is to explain why, in the same atmosphere and under the same illumination conditions, some objects grow dimmer and yellowish with distance, while others grow brighter and bluer. To do this we use a simple solution of the radiative-transfer equation and standard atmospheric-radiation codes to quantitatively evaluate a number of cases including objects that have a range of intrinsic colors. The results are presented as spectra and trajectories on the CIE chromaticity diagram.

In the discussion below, the term “color” refers to the CIE coordinates, and does not include the *perceived* effects of brightness, saturation, color contrast, field of view, visual context, adjacency effects, or optical illusions. By omitting these vast areas of perception from this paper, we are providing only the first step in a full understanding of how distant objects appear to the observer, i.e., a radiometrically based foundation from which broader perceptual studies might take their departure.

2. Objects Seen Through the Atmosphere

Throughout this paper, we will make frequent use of the results computed by MODTRAN4, a standard numerical atmospheric-radiance computer program.⁷ It is instructive, however, to first look at a simple solution to the radiative-transfer equation that illustrates many of the fundamental aspects of atmospheric color processes. The solution we will use is

$$I = I_0 e^{-\tau} + S(1 - e^{-\tau}), \text{ or } I/I_0 = e^{-\tau} + (1 - e^{-\tau})S/I_0, \quad (1)$$

where I is the observed spectrum, I_0 is the object’s intrinsic spectrum, S is the source function, and τ is the line of site (LOS) optical depth.^{8,9} The first term represents extinction, and the second term represents the airlight (Fig. 1). When $\tau = 0$ (completely clear), then $I = I_0$, and the object’s color appears without alteration. When $\tau = \infty$, then $I = S$, indicating that the original object is completely obscured and light from its direction has been replaced by integrated light from the source function. This is the case for the horizon brightness.³ In general, I_0 , S , and τ are functions of wavelength, but for the solutions shown in Fig. 1, we have done the calculation for a single (monochromatic), arbitrary wavelength.

As we shall see, the key to many colors lies in the source function. It is defined as

$$S = j/k,$$

where j is the emission coefficient and k is the ab-

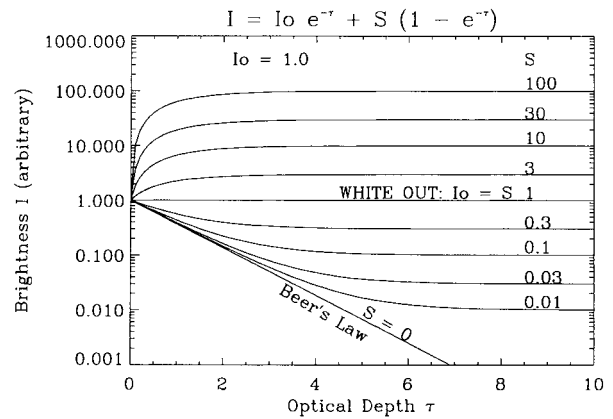


Fig. 1. Brightness I versus optical depth t of an object seen through an ideal, purely scattering atmosphere at an arbitrary wavelength. I_0 is the object’s intrinsic spectrum, and S is the source function. These are solutions of Eq. (1). When $\tau = 0$ (completely clear), then $I = I_0$ and the object’s color appears without alteration. When $\tau = \infty$, then $I = S$, indicating that the original object is completely obscured and light from its direction has been replaced by integrated light from the source function. Extinction or airlight may dominate depending on the ratio S/I_0 .

sorption coefficient. In this context, “emission” refers to the amount of light (usually sunlight) that is scattered into the line of sight from a unit volume. In general, j is usually similar to direct sunlight, but k is determined by Rayleigh scattering and the spectral properties of the aerosols along the LOS. Note that j and k have very different units, j being in (for example) $\text{W cm}^{-3} \mu\text{m}^{-1}$ and k being in cm^{-1} .

An important factor in Eq. (1) is the ratio of S/I_0 . If $S/I_0 \ll 1$ (bright object), then the airlight term will be negligible, and the object will grow dim and yellowish because of atmospheric extinction and Rayleigh scattering. The setting Sun is a good example. When $S/I_0 \gg 1$ (dark object), then the object will grow brighter and bluer as airlight is scattered into the LOS. Distant mountains show the effect clearly. An interesting case occurs when $I_0 = S$. This is the “whiteout,” where an object’s apparent brightness remains constant and the scene is without contrast.

There’s a curious aspect to Eq. (1) and Fig. 1. When extinction dominates, as it does if the source is bright, i.e., $I_0 \gg S$, then the e -folding optical depth is of order unity. But when the source is dark ($I_0 \ll S$), then the e -folding optical depth is much smaller. This happens because for small optical depths (and assuming $I_0 = 0$), the second term in Eq. (1) goes as

$$S(1 - e^{-\tau}) = S(1 - 1 + \tau - \tau^2/2! + \tau^3/3! \dots) \approx S\tau. \quad (2)$$

The brightness begins as low or zero and climbs rapidly in proportion to the product of $S\tau$. Thus the source function plays a major role in brightening with distance, and consequently $I(\tau)$ is dependent on the illumination of the scene. Extinction, on the other hand, is unaffected by illumination.

The calculations shown in Fig. 1 are parametric but they can be related to the physical world in the following way. Optical depth τ and LOS distance R (differential dR) through the atmosphere are related via

$$\tau(\lambda) = \int N(R)\sigma_T(\lambda)dR, \quad (3)$$

where N is the number density of scatterers and σ_T is the total scattering cross section. For a horizontal line of sight (LOS), Eq. (3) reduces to

$$\tau(\lambda) = RN\sigma_T(\lambda), \quad (4)$$

where R is the distance in km amagats. At STP with a horizontal LOS, amagat = 1. R is the distance in km and $N = \text{Loschmidt number} = 2.687 \times 10^{25} \text{ m}^{-3}$. The total cross section σ_T is the sum of the Rayleigh cross section σ_R and the aerosol cross section σ_A , each being a function of wavelength λ . The Rayleigh cross section of the average atmospheric molecule (mostly N_2 and O_2) is numerically represented by

$$\sigma_p = (4.16e^{-20})/\lambda^4 \text{ m}^2 \text{ molecule}^{-1}, \quad (5)$$

where λ is in nm. To get a feeling for the Rayleigh scattering optical depths and distances involved, a 1 km horizontal LOS at 500 nm has an optical depth of 0.0178. Alternatively, $\tau = 1$ when $R \approx 56 \text{ km}$. A vertical LOS from sea level (1 air mass) has an optical depth of about 0.15 at 500 nm.

3. Star Colors ($S = 0, \tau = 0$)

To set the stage for interpreting colors, we start with the most distant objects visible to the naked eye, stars.¹⁰ Stars emit thermal radiation. They have surface temperatures ranging from about 700 K for L and T stars^{11,12} to over 100 000 K for Wolf-Rayet stars.^{13,14} Stars hotter than about 4000 have blackbodylike spectra, but at progressively lower temperatures the spectra develop molecular absorption bands that cause their shape to depart significantly from a Planck function (Fig. 2). We shall assume that there is no atmospheric extinction ($\tau = 0$) and no source function ($S = 0$), reasonably valid assumptions in the visible for stars overhead. This assumption is equivalent to being outside the atmosphere and seeing the sources directly.

Figure 3 shows the CIE x - y trajectory of a series of blackbodies ranging from 1000 K to over a million degrees. Note that above about 20 000 K, the colors do not change perceptibly. This is because the radiation in the visible comes from the Rayleigh-Jeans tail of the Planck function, which is distributed as λ^{-4} . With the peak of the radiation falling in the ultraviolet, the relative distribution of the visible light does not change with temperature. The blackbody saturation colors in CIE coordinates are $x = 0.2404$ and $y = 0.2353$, in this case computed for a 10^6 K Planck function. This is in the "white" region of

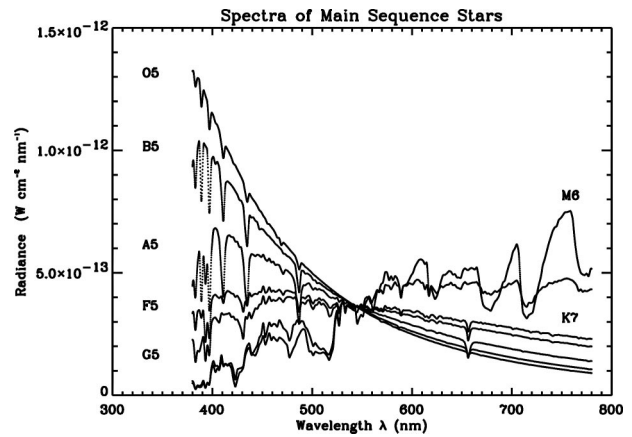


Fig. 2. Spectra of main sequence stars from Kurucz.¹⁶⁻¹⁸

Wysecki and Stiles,¹⁵ though on the blue side of it. Thus very hot objects appear white with a bluish tint.

Note that as the temperature of the blackbody decreases, the CIE colors move into a slightly yellowish-white region of the diagram before approaching the right-hand limit of the diagram. Owing to the absence of shorter wavelengths, the spectrum is growing narrower and more monochromatic. When the temperature has reached about 1500 K, the color is essentially indistinguishable from a monochromatic source.¹⁶

Figure 3 also shows the actual colors of main sequence stars (also called luminosity class V, or dwarf stars), computed from the stellar models of Kurucz.¹⁷⁻¹⁹ The blackbody and stellar colors agree above about 4000 K, but below this temperature the two curves separate for the reasons cited above. And despite the strong departures from a blackbody that cool stars show, they have little effect on the perceived color.

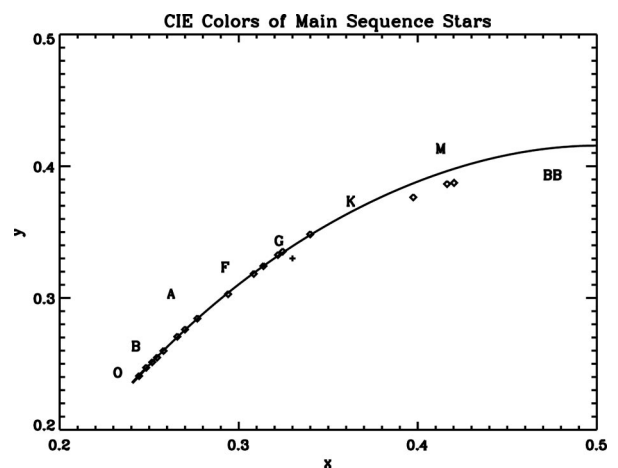


Fig. 3. CIE x - y trajectory of a series of blackbodies ranging from 1000 K to over a million degrees. Above about 20, 000 K, the colors do not change perceptibly. Also shown are the actual colors of main sequence stars from Fig. 3. Despite the strong departures from a blackbody that cool stars show, they have little effect on the perceived color.

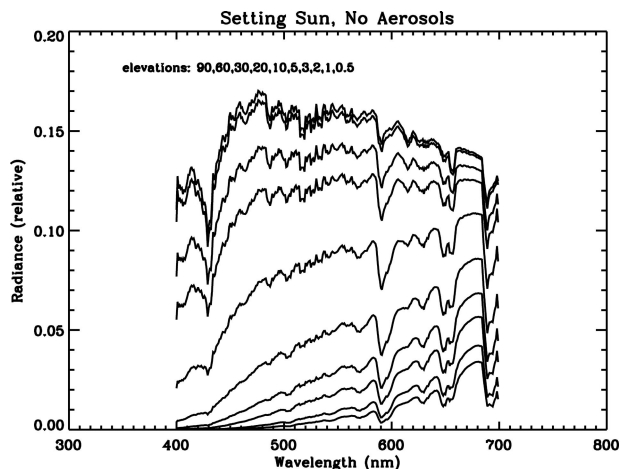


Fig. 4. Spectra of the Sun as a function of elevation angle for pure Rayleigh scattering. From top to bottom the spectra are for elevations 90, 60, 30, 20, 10, 5, 3, 2, 1, and 0.5 degrees. Near the zenith the solar spectrum ($W\text{ cm}^{-2}\text{ nm}^{-1}$) peaks near 500 nm, but at lower elevations the shorter wavelengths are attenuated more than the longer ones and the spectrum grows redder. Very near the horizon there is virtually no blue and very little green light.

The color trajectories never pass through regions of the CIE diagram corresponding to green, blue, or yellow. Only the orange region is penetrated, and only then just slightly. Thus the common examples of the overhead Sun and stars that are yellow (as in most paintings and childrens' drawings), green (because the solar spectrum is said to peak in the green²⁰ or blue (because they are "blue-hot") are wrong. As we will see in the next section, even when modified by the atmospheric transmission, the curves barely penetrate the yellow, green, or blue parts of the CIE diagram.²¹

4. Setting Sun ($S = 0$, or $S/I_0 \ll 1$)

Everyday experience tells us that when the Sun goes down, its color changes from white to yellow and sometimes orange or red. To quantify the colors, we computed the spectrum of the Sun as seen by an observer at sea level through a pure Rayleigh-scattering atmosphere (no aerosols, though MODTRAN does include molecular absorptions) using MODTRAN4 for a variety of solar elevations from 90° (zenith) to 0.5° (nearly on the horizon). The Sun was treated as a point source, and it is so bright ($S/I_0 \ll 1$) that we may safely ignore the sunlight scattered into the LOS (i.e., the airlight). The resulting spectra show the influence of Rayleigh scattering and atmospheric absorption, primarily by water vapor (Fig. 4). Near the zenith the solar spectrum ($W\text{ cm}^{-2}\text{ nm}^{-1}$) peaks near 500 nm, but at lower elevations the shorter wavelengths are attenuated more than the longer ones and the spectrum grows redder. Very near the horizon there is virtually no blue and very little green light. The CIE trajectory as a function of elevation is shown in Fig. 5. The colors are always slightly more yellow than those of a cooling blackbody (Fig. 3 above).

A more realistic atmosphere is represented by

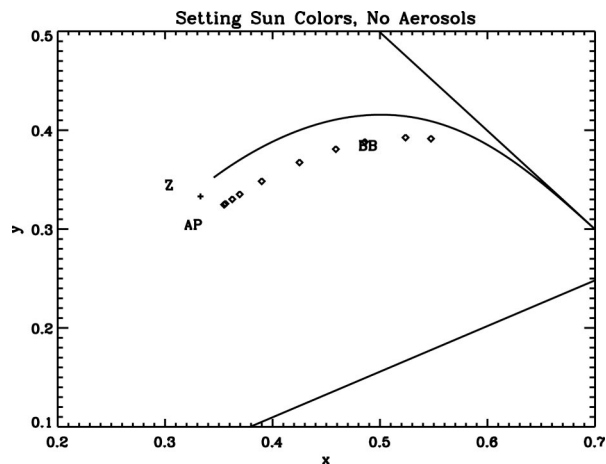


Fig. 5. Colors of the setting Sun in a pure Rayleigh-scattering atmosphere (from Fig. 5). From left to right the elevations of the Sun are 90, 60, 30, 20, 10, 5, 3, 2, 1, and 0.5 degrees. Also plotted is the trajectory of a cooling blackbody. Note that the Sun is always slightly more yellowish than a blackbody. Note that the high Sun is white and broadband, while the low Sun is red and much narrower across the spectrum. The colors are always slightly more yellow than those of blackbodies.

MODTRAN4's midlatitude summer for a visibility of 23 km, a fairly clear day. Such an atmosphere has boundary layer and stratospheric aerosols. The CIE colors of the setting Sun in this case are also shown in Fig. 6. Note that the presence of aerosols has a strong influence on the Sun's color, generally reddening it significantly over Rayleigh scattering. The reddening is relatively large despite the modest λ^{-1} dependence on aerosol scattering because of the large size of the particles compared to air molecules.

The color of the Sun varies most rapidly as it approaches the horizon. This is because the optical depth is proportional to the air mass (AM), the amount of air along the LOS ($AM = 1.0$ for the zenith). Air mass varies approximately as

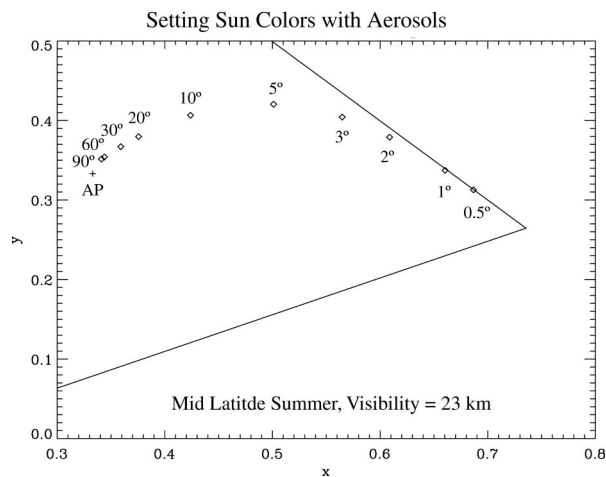


Fig. 6. Colors of the setting Sun in a relatively clear atmosphere (MODTRAN4, midlatitude summer, visibility of 23 km).

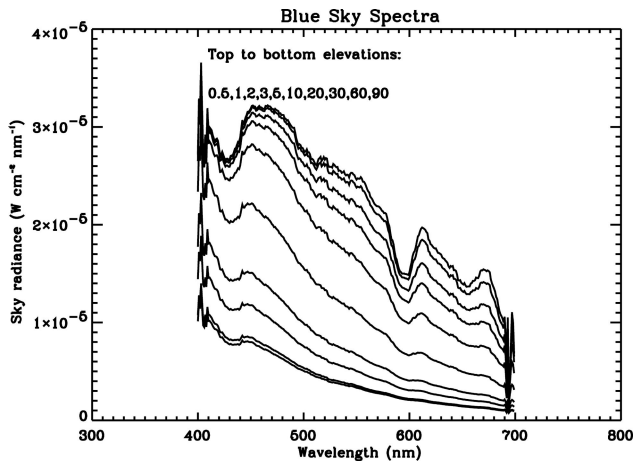


Fig. 7. Spectra of the sky computed by MODTRAN4 for a pure Rayleigh atmosphere. The sky is darkest and most colorful overhead (lowest curve) and whitest and brightest near the horizon (top curve).

$$\begin{aligned}
 AM = & \sec z - 0.0018167 * (\sec z - 1) \\
 & - 0.002875 * (\sec z - 1)^2 \\
 & - 0.0008083 * (\sec z - 1)^3, \quad (6)
 \end{aligned}$$

where z = zenith angle ($=90^\circ - \text{elevation}$).²² The often-observed low Sun with its upper portions bright yellow and its lower portion red and dim is a testament to the large change in air mass across its 0.5° vertical diameter near the horizon. In most cases, the color is determined by the aerosol content along the LOS, which is roughly proportional to air mass.

5. Color of the Sky ($I_o = 0$, or $S/I_o \gg 1$)

The sky's blue color varies with elevation.^{23–26} Ignoring the Sun and aureole,^{27,28} it is darkest and bluest overhead and gradually brightens and whitens as the LOS approaches the horizon. Relative to the Sun, there is an azimuthal component of this color and brightness as a result of scattering. The spectra of the sky computed by MODTRAN4 for a pure Rayleigh atmosphere are shown in Fig. 7. The corresponding CIE colors are shown in Fig. 8. It is clear from the spectra that blue sky light is broadband and contains significant amount of light from every wavelength in the visible spectrum. Thus it is not surprising to find that the perceived color is only slightly bluish and far from saturated.

6. Black and White Objects on the Horizon

The limiting cases of resolved black and white objects (0 and 100% reflectivity, respectively) at all visible wavelengths provide much of the basis for understanding the colors of distant objects. Examples of natural sources that approximate these two extremes are dark mountains (reflectivity about 4%) and snow capped mountains or thick clouds (reflective near unity).

Consider a totally black object ($I_o = 0$) viewed horizontally from sea level at a variety of distances. For

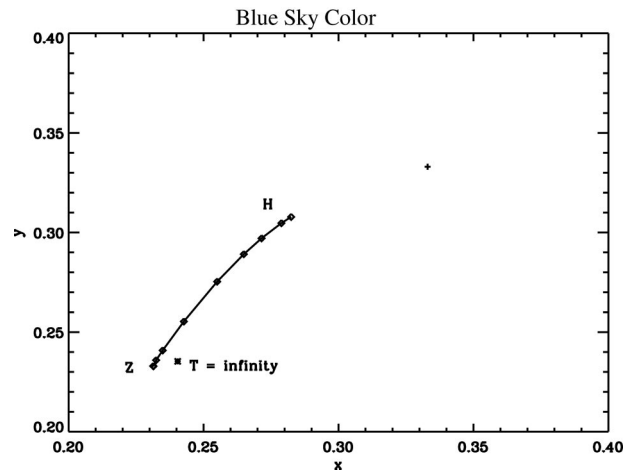


Fig. 8. CIE colors of the spectra in Fig. 7. Near the horizon H, the sky is very close to being ideal white, i.e., near the achromatic point. Overhead at the zenith (Z) the sky is bluer than the hottest blackbody, though still far from saturated.

this case we have selected distances corresponding to optical depths and distances shown below, though naturally we have included the wavelength-dependent optical depth in the calculations:

500 nm optical depth	distance (km)
0.01	0.6
0.03	1.7
0.1	5.6
0.3	16.8
1	56
3	167
10	559

We have approximated the source function S as a 5700 K blackbody spectrum scaled to the solar constant, a close approximation of the solar spectrum. Using the smooth blackbody spectrum avoids the distraction of spectral structure present in the true solar spectrum. Figure 9 shows the observed spectra, and Fig. 10 shows the colors.

A white object like a distant cloud, on the other hand, has a nonzero intrinsic brightness I_o , so we must include both terms from Eq. (1) in the computations. Furthermore, we must make some adjustment for anisotropic scattering in the computation because sunlight scattered into the beam (airlight) has different properties than light scattered out of the LOS (extinction). If we assume that the Sun is overhead and that the LOS is horizontal, then the Rayleigh-scattered airlight term will be less than the extinction term because Rayleigh scattering is near its minimum for a 90 degree scattering angle. To demonstrate the effect, we adopt the relation $S = I_o * A$, where A is a scaling parameter that is always less than unity. The resulting spectra are shown in Fig. 11, and the corresponding colors are shown in Fig. 12 for a value of $A = 0.5$.

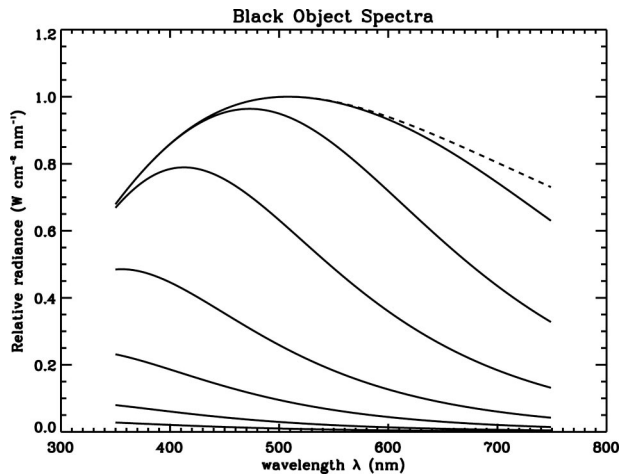


Fig. 9. CIE spectra of a black object viewed at various distances (optical depths from bottom to top are 0.01, 0.03, 0.1, 0.3, 1, 3, 10) with a horizontal LOS. The object begins faint and faintly blue (bottom curve). With increasing distance, the object appears to grow brighter and whiter until at very large distances it is spectral identical to the source function, in this case the 5700 K blackbody approximating the color spectrum.

Here we see something odd. With increasing optical depth, the cloud initially grows slightly reddish or pink, then reverses direction and grows bluer until it returns to a final color that in this case is indistinguishable from its original color. The final color does not represent its original color, but rather the color of the distant horizon sky. This is because we used the same color for both the cloud and the source function, i.e., a 5700 K blackbody. It does, however, closely mimic the apparent color changes in real clouds in a real atmosphere.

The interpretation of this reversing route is consistent with observations. The colors of distant clouds illuminated by a near-zenith Sun never appear as deep, saturated red. In fact, at their most colorful, they are very faintly pink, and only then when the optical depth to them is of order 3. For optical depths

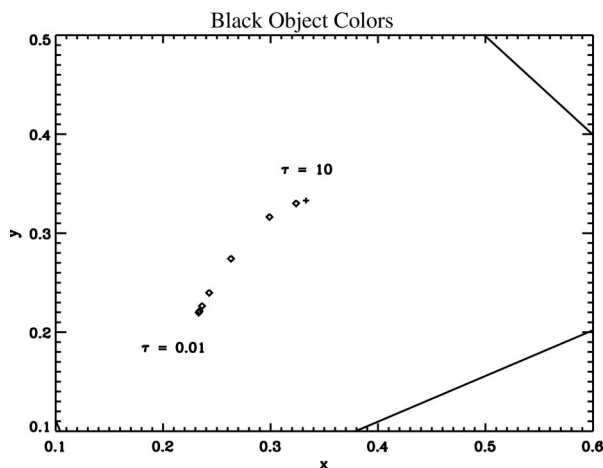


Fig. 10. Colors of the spectra from Fig. 10.

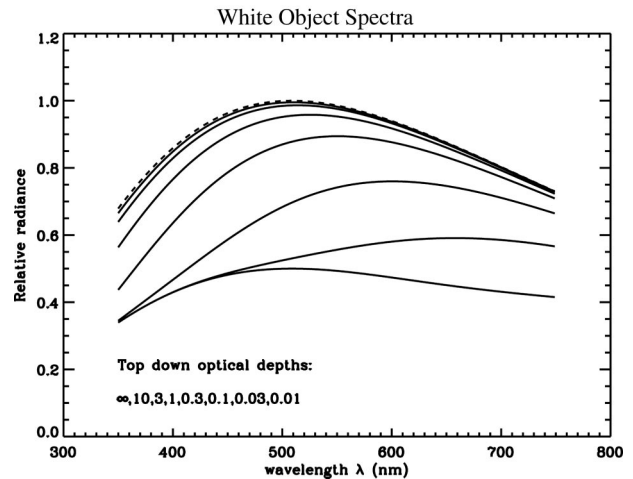


Fig. 11. Spectra of a white object at various distances through the atmosphere for a value of $A = 0.5$.

below 3, they tend to appear fairly white, and above 3 faintly pink or invisible.

We have now quantitatively explained the apparent colors of two common distant objects: clouds and mountains (light and dark, respectively, corresponding to Fig. 10 and 12). The final step is to examine the role of brightness in the perception of colored sources with distance. We selected six notch or “square wave” spectra that were zero at all wavelengths except in a specified region where the brightness is unity. The colors ranged from deep blue to deep red, each about 30 nm wide. By multiplying the brightness by $A = S/I_0$, we have a convenient way of choosing sources that are very bright compared to the landscape ($S/I_0 < 1$) or dim ($S/I_0 > 1$).

Figures 13, 14, and 15 show the apparent color trajectories for a number of colorful objects seen at distances corresponding to the 500 nm optical depths given above. The colors start out on the periphery of the chromaticity diagram and move toward the center with increasing optical depth. For small optical depths, the colors are essentially unchanged from

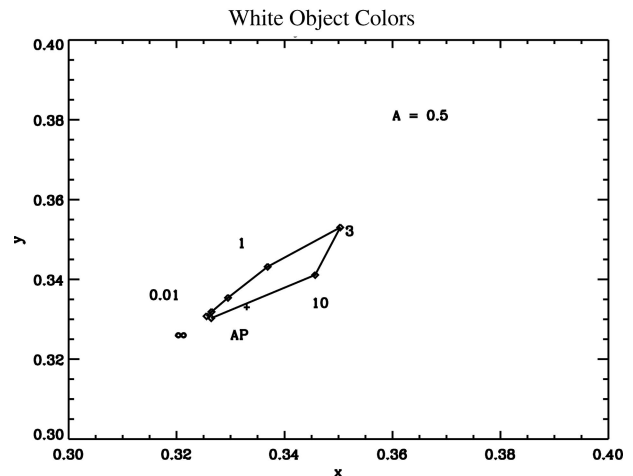


Fig. 12. CIE colors corresponding to the spectra from Fig. 12.

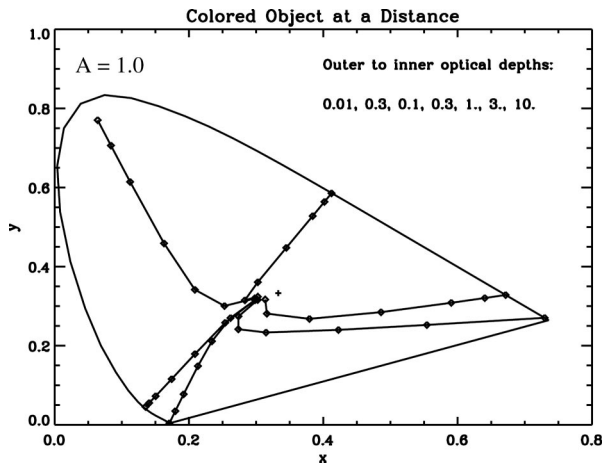


Fig. 13. CIE of six colors for $A = 1.0$ (bright-colored reflective paper).

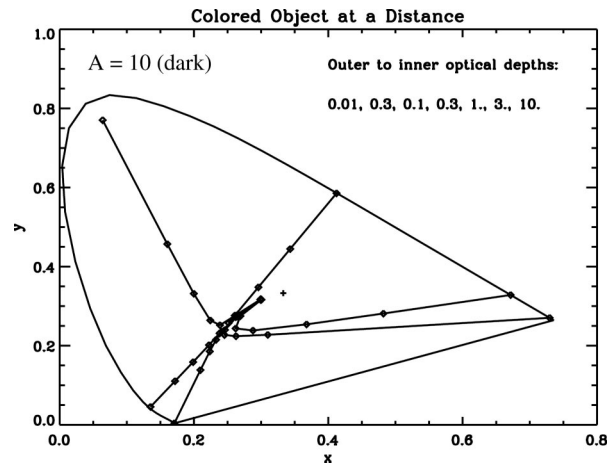


Fig. 14. CIE of six colors for $A = 10.0$ (dark-colored rocks).

their intrinsic values, and at large optical depths they approach but do not reach the achromatic point, not that they necessarily should. The effect of brightness (A) is to control the rate at which they move toward the center, i.e., the rate at which the colors desaturate. For dark objects ($A = 10$, Fig. 14) the colors rapidly shift from the edge of the chromaticity diagram because the objects are intrinsically faint and airlight quickly comes to dominate the colors. This is why they move toward the blue side of the diagram before turning around and approaching the achromatic point. For bright objects, however ($A = 0.1$, Fig. 15), the sources stick to their true colors longer because the airlight has a relatively smaller effect on them. As a result, they trend more directly toward the achromatic point without detouring through the airlight-dominated blue side of the diagram.

7. Discussion

Brightness is important to visibility and color, but it is normalized out when computing CIE coordinates. But it is important to recognize that we never see a deep red cloud when the Sun is high as in the simulations. This is because at sufficiently large distances (optical depths), the cloud's brightness is heavily attenuated to the point of invisibility. Only the brightest sources can shine through an optical depth of 3 or more, especially in the presence of airlight. This is why distant snow-capped peaks and clouds are seldom redder than pale pink. When they are farther away, they are too faint to be seen. The same is true of dark mountains: With increasing distance (optical depth) they grow brighter and bluer, and eventually they merge with the white atmosphere at the horizon. Aerosols are also important and in most cases represent the dominant source of opacity. They have a broader, less colorful attenuation and scattering spectrum, and as a result they add a "whitish" opacity and "whitish" airlight to the scene.

The analyses above are based only on the shape of the radiometric spectra and do not include physiological perception effects. Perception modifies the appar-

ent colors for a variety of reasons. Many stars that are easily visible to the naked eye are too faint to elicit a color response in the eye. Viewed through a telescope, such stars will show their true color. Yet if the star is bright enough or the telescope large enough, the brightness will saturate the color receptors and the star will appear white, regardless of the shape of its spectrum. The same, of course, would be true if the observer were close enough to the star to resolve it, as we are in the case of the Sun.

Color contrast can also play a role in the perceived color. For example, Albireo (β Cygni) is a double star, the components being a 3.1 magnitude K3 supergiant (4200 K) and a 5.1 magnitude B9.5 dwarf (10, 500 K). The pair is often described as "topaz yellow and sapphire blue." As shown above, such appellations are not realistic, but the strong color contrast when viewed against a dark background seems to accentuate the stars' colors.²⁹

The fact that bright stars elicit a color response in the eye is not well understood. With illuminance levels around 10^{-6} lumen m^{-2} , they fall well within the range of scotopic vision, and scotopic vision does not

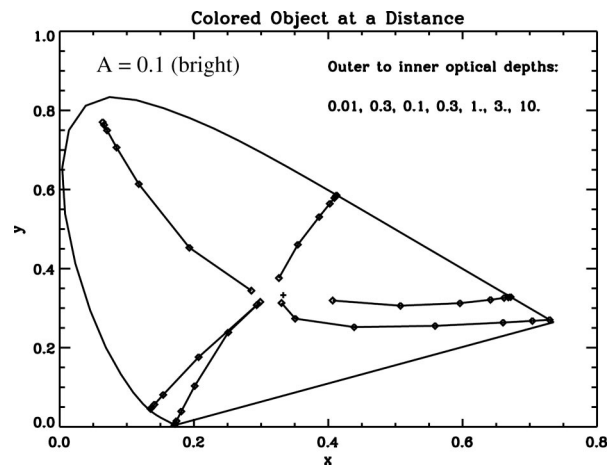


Fig. 15. CIE of six colors for $A = 0.1$ (bright self-luminous sources like city lights).

support color perception. And yet, as Fig. 4 would suggest, Betelgeuse ($T = 3000$ K) appears distinctly orange, Arcturus ($T = 4000$ K) a creamy yellow, and Sirius ($T = 9800$ K) white with a bluish tint. How is this possible? We have three speculations that we will state but not explore in this paper: (1) Perhaps there is some cross talk between scotopic and photopic vision for sources that are smaller than the diffraction limit of the eye, i.e., point sources, especially against a dark background. (2) There might be enough airlight and other light from the night sky to raise the illuminance level to mesopic or low photopic levels. (3) In the case of very red stars, the blue end of the spectrum may be at scotopic levels, but the red end may be mesopic or photopic. Whatever the answer turns out to be, it is undeniable that the unaided, dark-adapted eye can perceive star colors that seem to qualitatively match the values one might expect from a bright (photopic) object with the same radiometric spectrum.

The Sun is white. Despite a massive literature on the subject, everyone from kindergarten teachers to scientists who should know better continue to perpetuate the notion that the Sun is yellow. Near the horizon, maybe, or through smoke perhaps, but not overhead and not from space. "White," of course, is a matter of definition. In the context of the chromaticity diagram, white is defined only at a single point, the achromatic point (AP in Figs. 1, 2, 4, 6, 7, 9, 11, and 12), where all three tristimulus values have the same value. This occurs at $x = 0.333$ and $y = 0.333$. Other color systems use other definitions, and the actual location of the AP depends upon the illumination source.

For pure Rayleigh scattering the color of the horizon sky is white. Aerosols also lead to a white horizon sky but at much smaller distances, owing to their effect of increasing the optical depth compared to pure Rayleigh scattering. The actual color of the horizon sky can take on various tints as a result of reflection of light from the landscape: desert horizon may be slightly brownish, jungle horizons greenish, and ocean horizons bluish,²⁷ an effect called "blinks."

8. Color Perception in the Real World

Having a radiometrically calibrated spectrum and its corresponding CIE coordinates does not tell us what the observer actually perceives. As an example (of which there are many), consider this remark by Minnaert³⁰ concerning the colors of distant objects:

"Now look at the distant landscape. It appears to be covered by a light haze, mostly bluish in hue, which is caused by dispersion in the air and dust particles. It is peculiar that we hardly noticed the haze when we looked at the landscape as a whole. In the mountains we often see a slope as grayish or brownish, covered here and there by a patch of green trees. Looking through the funnel, however, we notice that the entire slope is really blue, as are the trees, although the slope is slightly darker and bluish gray, whereas the trees are greenish blue. It

*seems as if we are subconsciously trying to remove a homogeneous veil from the whole landscape."*²⁹

Henry *et al.*³¹ show that the color that a spectrograph might measure (i.e., CIE coordinates as in this paper) is significantly different than the color a human observer might ascribe to a scene by using color-matching cards (the so-called transparency effect). The results depend on their field of view: when looking through a narrow tube, observers report a strong blue color, but when looking at the entire scene and seeing the distant object in context, they perceive colors closer to the ones that they know are present in the absence of airlight. The reasons, of course, are complex and not entirely understood. We mention this example to reinforce the notion that radiometrically calibrated spectra are the first steps in understanding color perception, not the last.

9. Summary and Conclusions

We have presented CIE colors for a variety of natural objects viewed under a range of atmospheric conditions. These colors were derived by converting the spectra to 1931 CIE chromaticity coordinates. The main conclusions are:

1. The intrinsic colors of stars are largely achromatic, with only the coolest having deeply reddish colors and the hottest having very slightly bluish colors. The Sun is white. Greens are never seen, nor are rich, deeply saturated colors except red. The non-Planckian spectra of very cool stars have little effect on their perceived colors when compared to colors of blackbodies.
2. The setting Sun's colors approximate the colors of blackbodies, though they are slightly more yellow. Deeply saturated reds and oranges do occur for low Sun elevations. The presence of aerosols heavily influences the colors of the Sun.
3. The sky's blue color is not highly saturated. It is only slightly bluer than very hot objects ($T = 10^6$ K). Near the horizon, the sky is essentially white, i.e., achromatic.
4. The trajectories of most natural objects' colors as a function of distance describe two narrowly confined paths in the CIE diagram, red trending and blue trending.

We would like to thank Kenneth Brecher for useful discussions regarding the colors of stars, both real and perceived. We are grateful to Middleton and his book *Vision Through The Atmosphere* for setting forth a sound, clear foundation of the colors of distant objects. This paper follows Middleton's approach, later extended by Raymond Lee, Jr., and his colleagues. The author is indebted to a referee for drawing his attention to Minnaert's 1953 paper.³⁰

References

1. Lord Rayleigh (J. W. Strutt), "On the light from the sky, its polarization and colour," *Philos. Mag.* **41**, 107, 274 (1871).
2. K. Middleton, *Vision Through the Atmosphere* (University of Toronto Press, 1952).

3. E. J. McCartney, *Optics of the Atmosphere* (Wiley, New York, 1976).
4. C. Bohren, "Multiple scattering of light and some of its observable consequences," *Am. J. Phys.* **55**, 524–533 (1987).
5. <http://www.cie.co.at/cie/>.
6. M. Fairchild, *Color Appearance Models* (Addison-Wesley, Reading, Mass., 1998).
7. L. Berk, L. S. Bernstein, and D. C. Robertson, "MODTRAN: a moderate resolution model for LOWTRAN7," Air Force Geophysical Laboratory Tech. Rep. GL-TR-89-0122 (Hanscom Air Force Base, Mass., 1989).
8. W. Kalkofen, ed., *Methods in Radiative Transfer* (Cambridge University, Cambridge, 1984).
9. W. Kalkofen, ed., *Numerical Radiative Transfer* (Cambridge University, Cambridge, 1987).
10. There are a few galaxies that are visible to the naked eye, and they are more distant than the stars. But they are too faint to elicit a color response in the eye.
11. A. J. Burgasser, J. D. Kirkpatrick, M. E. Brown, I. N. Reid, J. E. Gizis, C. C. Dahn, D. G. Monet, C. A. Beichman, J. Liebert, R. M. Cutri, and M. F. Skrutskie, "Discovery of four field methane (T-type) dwarfs with the two micron all-sky survey," *Astrophys. J.* **522**, L65–L68 (1999).
12. J. D. Kirkpatrick, I. N. Reid, J. Liebert, R. M. Cutri, B. Nelson, C. A. Beichman, C. C. Dahn, D. G. Monet, J. E. Gizis, and M. F. Skrutskie, "Dwarfs cooler than "M": the definition of spectral type "L" using discoveries from the 2 micron all-sky survey (2MASS)," *Astrophys. J.* **519**, 802–833 (1999).
13. C. J. Wolf and G. Rayet, *Comptes Rendus Acad. Sci.* **65**, 292 (1867).
14. W. R. Hamann, L. Koesterke, and U. Wessolowski, "Spectra analysis of the galactic Wolf–Rayet stars—a comprehensive study of the WN class," *Astron. Astrophys.* **274**, 397 (1993).
15. G. Wysecki and W. S. Stiles, *Color Science* (Wiley, New York, 1967).
16. There is another reason that very hot and very cool sources appear to be the same color regardless of temperature: At the extreme wavelength limits of human vision, most of the light is exciting only the red or blue rhodopsin. Color discrimination depends on the relative ratios of the R, G, and B rhodopsins, and when only one is excited, only one color is seen.
17. R. L. Kurucz, in *Atomic Spectra and Oscillator strengths for Astrophysics and Fusion Research*, J. R. Hansen, ed. (North-Holland, Amsterdam), p. 20.
18. R. L. Kurucz, in *Stellar Atmospheres: Beyond Classical Models*, L. Crivellari, I. Hubeny, and D. G. Hummer, eds., NATO ASI Ser. C **341**, (1991), p. 441.
19. R. L. Kurucz, in *The Stellar Populations of Galaxies*, B. Barbuy and A. Renzini, eds., *Int. Astron. Union Symp.* **149**, 225 (1992).
20. B. H. Soffer and D. K. Lynch, "Some paradoxes, errors and resolutions concerning the spectral optimization of human vision," *Am. J. Phys.* **67**, 946 (1999).
21. These results are substantially the same for giant and supergiant stars, which tend to be the ones that are brightest in the night sky. Most stars in the galaxy are faint red dwarfs, but the brightest stars, i.e., the ones visible from the greatest distance, are giants and supergiants.
22. W. Romanishin, *An Introduction to Astronomical Photometry Using CCDs* www.nhn.ou.edu/~wjr/research/wrccded2.pdf (1999).
23. R. L. Lee, Jr., "Twilight and daytime colors of the clear sky," *Appl. Opt.* **33**, 4629–4638 4959 (1994).
24. J. Hernández-Andrés, R. L. Lee, Jr., and J. Romero, "Calculating correlated color temperatures across the entire gamut of daylight and skylight chromaticities," *Appl. Opt.* **38**, 5703–5709 (1999).
25. J. Hernández-Andrés and R. L. Lee, Jr., "Color and luminance asymmetries in the clear sky," *Appl. Opt.* **42**, 458–464 (2003).
26. M. A. Box and A. Deepak, "Retrieval of aerosol size distribution by inversion of solar aureole data in the presence of multiple scattering," *Appl. Opt.* **18**, 1376–1382 (1979).
27. J. T. Twitty, "The inversion of aureole measurements to derive aerosol size distribution," *J. Atmos. Sci.* **32**, 584–591 (1975).
28. D. K. Lynch and W. Livingston, *Color and Light in Nature* (Cambridge University, Cambridge, 2001).
29. L. Bell, "Star colors: a study in physiological optics," *Astrophys. J.* **31**, 234–257 (1910).
30. M. Minnaert, "Colour and colour perception," *Proc. Acad. Amsterdam B* **56**, 148 (1953).
31. R. C. Henry, S. Mahadev, S. Urquijo, and D. Chitwood, "Color perception through atmospheric haze," *J. Opt. Soc. Am. A* **17**, 831–835 (2000).